Technium Vol. 2, Issue 7 pp.143-150 (2020)
ISSN: 2668-778X
www.techniumscience.com

Study on the Synthesis and Photocatalytic Performance of Tube shaped Activated Carbon -TiO_2 Composite Materials

Zhifu Wu
School of Pharmacy, Guilin Medical University, Guilin, Guangxi, 541199, China
Corresponding email: 1772716011@qq.com

Abstract: Titanium dioxide semiconductor material is one of the earliest photocatalysts with stable and reliable properties, but its quantum efficiency is relatively low. In order to improve the photocatalytic performance of titanium dioxide, the activated carbon tubular-titanium dioxide composite photocatalytic material was synthesized by sol-gel method with n-butyl titanate and activated carbon as main raw materials in the system of isopropyl alcohol and glacial acetic acid. X-ray diffraction (XRD), scanning electron microscope (SEM) and nitrogen adsorption were used to characterize the phase, particle size and adsorption performance of the photocatalyst. The photocatalytic performance of the synthesized material was tested by using rhodamine B, a simulated pollutant. The results show that rhodamine B decomposition rate can reach 100% under UV irradiation for 140 minutes. The conclusion is that the photocatalytic performance of the activated carbon tube interspersed with titanium dioxide composite was significantly improved.

Key words: Tube shaped activated carbon, Sol-gel method, Rhodamine B, Photocatalyst

1.Introduction

In recent years, photocatalytic technology has been particularly favored with the increasing environmental pollution [1]. Titanium dioxide semiconductor materials have advantages that other semiconductor materials do not have, such as stable chemical properties, good electronic conductivity, high efficiency, non-toxic and good biocompatibility, which make them a hot research spot at home and abroad [2-5]. However , due to the wide energy band gap of TiO_2 (the anatase is 3.20 ev , and the rutile TiO_2 is 3.02 ev) [6] , the photogenerated

electron-hole pairs are easy to compound , resulting in low quantum efficiency , which limits the effective utilization of this material for visible light [7] .

Domestic and foreign scientists try to composite mesoporous carbon materials and titanium dioxide, combine photocatalytic technology and adsorption technology to achieve rapid transfer of photogenerated electrons, thereby improving the photocatalytic efficiency of the composite system [8]. The small size effect and quantum effect of carbon nanotubes can effectively improve the photocatalytic performance and photoelectric conversion efficiency of TiO_2 [9]. However, because carbon nanotubes are relatively expensive, it is necessary to find a cheap alternative material. Some studies have shown that activated carbon is expected to replace carbon nanotubes to reduce costs [10]. The composite process of activated carbon and titanium dioxide is simple and green. In this experiment, activated carbon tube / TiO_2 photocatalytic material was synthesized by sol-gel method. The photocatalytic performance of the synthesized material was studied by using the simulated pollutant rhodamine B.

2. Experiment

2.1. Instruments and reagents

N-butyl titanate (Shandong Heruidong Fine Chemicals Co , Ltd) ; Rhodamine B (Shanghai Aladdin Biochemical Technology Co , Ltd) ; Isopropanol (Sinopharm Chemical Reagent Beijing Co , Ltd) ; C_2H_5OH (Sinopharm Chemical Reagent Beijing Co , Ltd) ; Ice acetic acid (Sinopharm Chemical Reagent Beijing Co . , Ltd .) ; Activated carbon (Sinopharm Chemical Reagent Beijing Co , Ltd) ; HNO_3 (Guangdong Guanghua Technology Co . , Ltd .) , above reagents are analytically pure . The experimental water is secondary distilled water .

Constant temperature magnetic stirrer ; ultrasonic cleaner ; muffle furnace ; UV-1600 dual-beam UV-visible spectrophotometer (Shimadzu , Japan) , power of 120 W UV lamp . All-intelligent high-power Smart lab 2006 X-ray diffractometer (Japanese Science Society) ; SU-8010 field emission scanning electron microscope (Hitachi , Japan) .

2.2. Preparation of composite materials

The first step: 0.4 g activated carbon was dispersed in 80 mL 80 % ethanol solution and shaken in ultrasonic cleaner for 1 hour. The second step : 5 mL isopropanol and 5 mL n - butyl titanate mixed evenly ; The third step : 10 mL glacial acetic acid was added into the solution prepared in the first step , and then the solution obtained in the second step was added into the mixed solution at the rate of 20 drops per minute in the ice water bath. After the addition, the ice water bath was removed and stirred for 6 hours at room temperature. Then the solution was distilled into viscous form at 70 °C and refluxed for 8 hours . The viscous substance was taken out and dried in vacuum at 65 °C for 5 hours. Then the solid was ground and calcined at 480 °C , 580 °C , 680 °C and 780 °C for 2 hours to obtain four products .

Technium Vol. 2, Issue 7 pp.143-150 (2020)
ISSN: 2668-778X
www.techniumscience.com

2.3. Photocatalytic degradation experiment

The catalytic performance of activated carbon tube-TiO_2 composite powder was measured with rhodamine B solution as simulated pollutant . The typical experimental process was as follows : 10 mg Rhodamine B was dissolved in 100 mL secondary distilled water to form 100 mg / L Rhodamine B aqueous solution . Ten mg of the four powders prepared in the experiment were weighed and put into four beakers , respectively. Then 20 ml of rhodamine B was added into each beaker , numbered as 1 , 2 , 3 and 4. In the absence of light environment using magnetic stirrer stirring for 10 minutes , the photocatalyst and rhodamine B adsorption balance . The UV catalytic decomposition instrument was used for degradation , and the samples were taken every 20 minutes , and the absorption curve was detected by UV spectrophotometry after centrifugal separation.

3. Results and analysis

3.1. Phase analysis

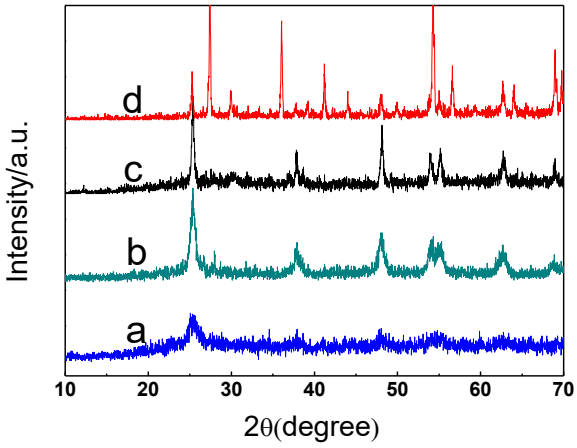

Fig.1 XRD pattern of as the prepared products at different calcination temperatures (calcination temperature a: 480 ℃, b: 580 ℃, c: 680 ℃, d: 780 ℃)

Fig1 shows the XRD patterns of the products obtained at different calcination temperatures . In curve a , the sample calcined at 480 ℃ showed the characteristic diffraction of anatase phase (101) at 2θ = 25.1° , corresponding to PDF standard card (JCPDS) 71 – 1169 . Although the crystallinity was poor , it was preliminarily estimated to be anatase . With the increase of calcination temperature , other characteristic diffraction peaks of anatase phase appear , and the strength increases with the increase of calcination temperature , indicating that the crystallinity of the sample increases with the increase of temperature . When the calcination temperature reached 580 ℃ and 680 ℃ , the spectrum showed a typical anatase diffraction peak , and the diffraction peaks at 2θ were 25.1° , 37.4° , 48.2° , 54.1° and 55° , respectively , belonging to the anatase TiO_2 crystal plane , corresponding to PDF standard card (JCPDS) 84

- 1286 ; When the calcination temperature is less than 680 °C , the products are anatase , and there is no transformation of rutile . The curve d indicates the XRD pattern of anatase phase to rutile phase when the calcination temperature is greater than 680 °C . It can be seen from the figure that most TiO_2 is transformed from anatase phase to rutile phase at this temperature , corresponding to PDF standard card (JCPDS) 73 - 1232.

3.2. Surface Morphology Analysis of Products

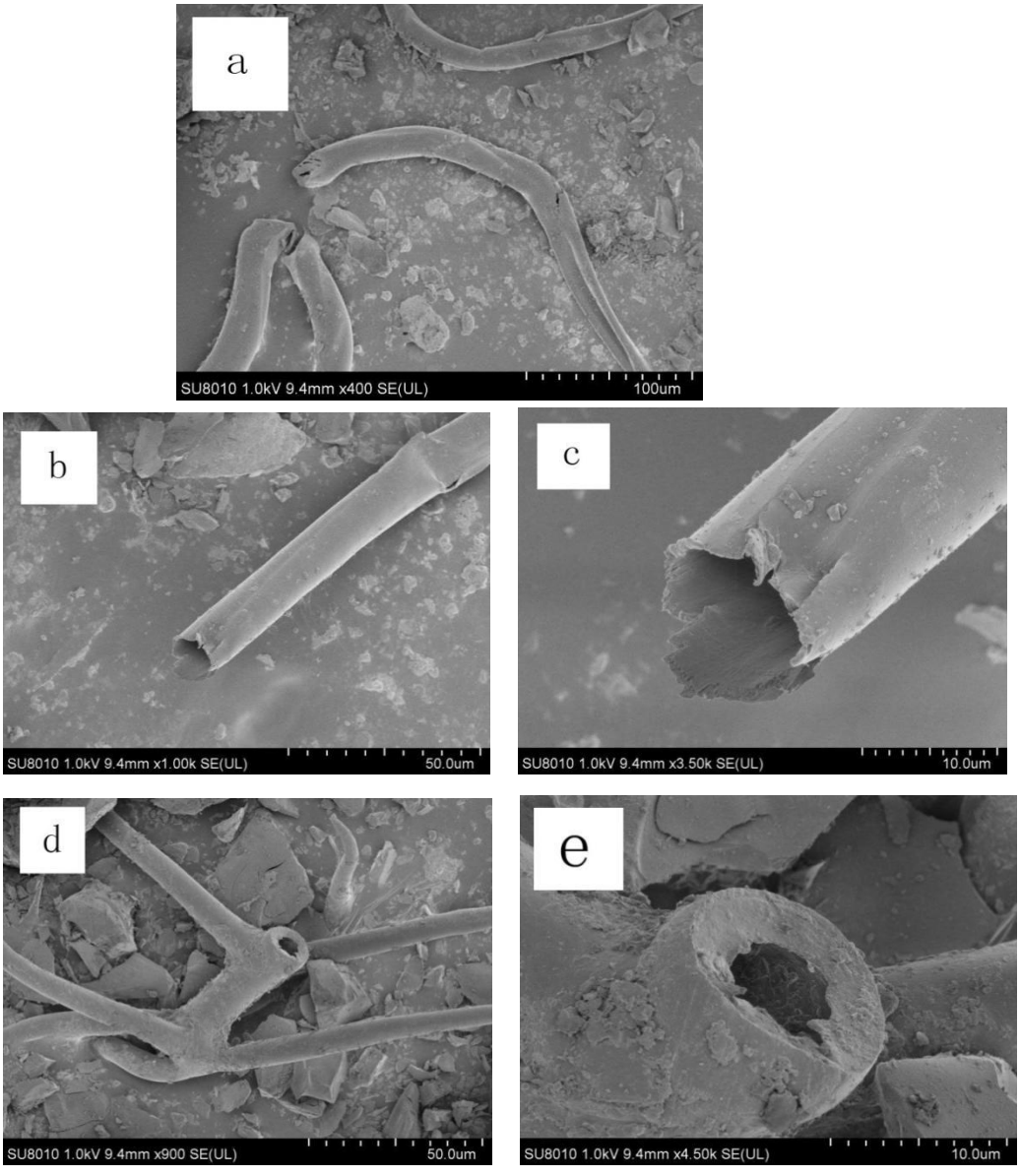

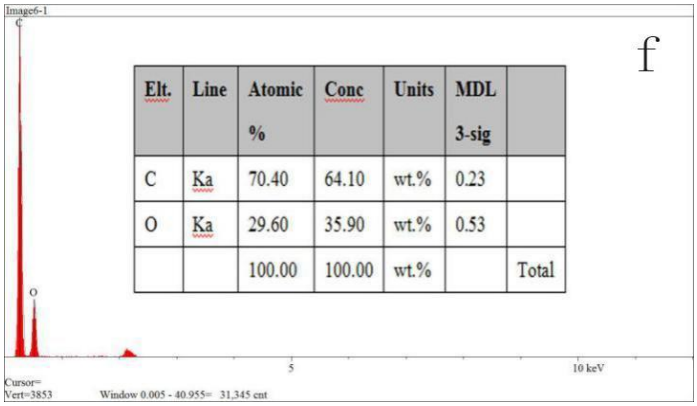

Elt.	Line	Atomic %	Conc	Units	MDL 3-sig	
C	Ka	70.40	64.10	wt.%	0.23	
O	Ka	29.60	35.90	wt.%	0.53	
		100.00	100.00	wt.%		Total

Fig. 2 SEM images and EDS of the synthesized sample calcined at 580 ℃ (magnification a:×400, b: ×1.00k, c: ×3.50k, d: ×900, e: ×4.50k)

Fig . 2 shows the SEM and EDS of the synthesized samples calcined at 580 ℃ . Fig . 2a shows a scanning electron microscope image with a magnification of 400 times. It shows that there are four root canals , with a curve distribution and uniform size. The longest tube is about 280 μm , and there are massive particles around it. Fig .2b is the local enlargement of a single pipe in Fig . 2a and Fig . 2c is the local enlargement of Fig. 2b. The diameter of the pipe is 14.4μm . Fig . 2d is a material structure diagram with branch pipe . The diameter of the main pipe channel is 16 μm , with multiple lateral branches , and the block is evenly distributed next to it. Fig. 2e shows the local enlargement of Fig. 2d. The thickness of carbon tube is 4 μm. Fig. 2f shows the energy spectrum of the material . XRD and EDS analysis showed that the chemical composition of these microtubes was composed of C elements , and the bulk particles were TiO_2.

3.3. Nitrogen adsorption experiment

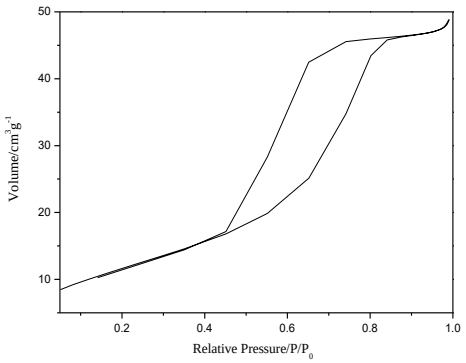

Fig. 3 BET diagram of the photocatalyst synthesized at 580℃

In order to further understand the synthesis of adsorption properties and pore distribution, we to the calcination temperature is 580℃ when samples synthesis by the nitrogen adsorption

experiment, figure 3 is the nitrogen adsorption isotherm, curve in the figure shows a broad hysteresis ring, according to the IUPAC classification, the curve as part of the first IVisotherm [11], that the materials of mesoporous materials, under the low relative pressure, monolayer adsorption; At high relative pressure, the adsorbents produced capillary condensation. When the relative pressure was 0.48~0.82, the adsorption and desorption curves were separated. After condensation of all the pores, the adsorption only occurred on the surface far less than the surface area, and the curve was flat. When the relative pressure is close to 1, the adsorption on the macropore increases the curve.

3.4. Analysis of photocatalysis results

FIG. 4 shows the UV spectra of rhodamine B degradation by photocatalyst prepared at 580℃.It can be seen from the figure that rhodamine B is chemically stable without photocatalyst.

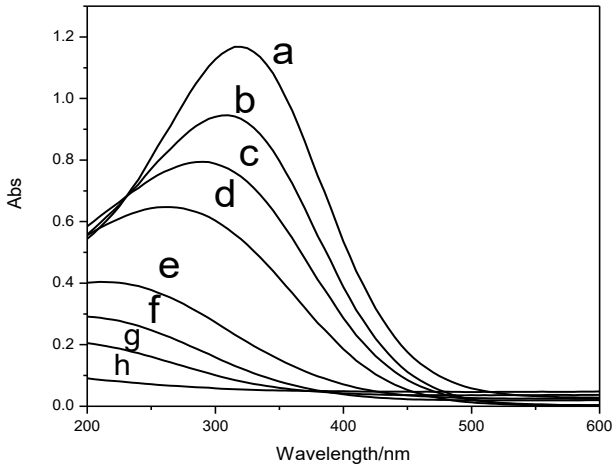

Fig. 4 Photocatalytic degradation curve of rhodamine B by composite materials synthesized at 580 ℃.

Curve a is the absorbance of rhodamine solution to reach adsorption equilibrium after adding photocatalyst for 10 minutes. b, c, d, e, f, g and h are the absorbance curves of photocatalytic degradation after 20, 40, 60, 80, 100, 120 and 140 minutes in turn. With the prolongation of photocatalysis time, it can be seen that the peak value of the curve gradually decreases, and the color of rhodamine B gradually becomes lighter until it decreases completely after 140 minutes, and the solution becomes colorless. This indicates that the photocatalyst has a good degradation effect on rhodamine B. Similar parallel experiments show that the photocatalytic effect sequence of the composite prepared at different temperatures is: 580℃ > 680℃ > 480℃ > 780℃.

3.5. Photocatalytic mechanism

Activated carbon tube has obvious advantages in adsorption due to its unique void structure and the presence of surface active groups. Activated carbon tube has a strong

adsorption of rhodamine B, but it can't be used again until it is regenerated after adsorption saturation. TiO_2 and activated carbon were controlled to form a composite photocatalyst, which could combine the photocatalytic activity of TiO_2 with the adsorption performance of activated carbon tube. On the one hand, the strong adsorption of activated carbon tube provides a high concentration reaction environment for the photocatalysis of TiO_2, which speeds up the reaction speed and improves the reaction efficiency. On the other hand, under the action of ultraviolet light, TiO_2 photocatalysis degrades the adsorbed rhodamine B to regenerate the activated carbon tube. The photocatalytic mechanism of activated carbon tube- TiO_2 composite material is as follows:

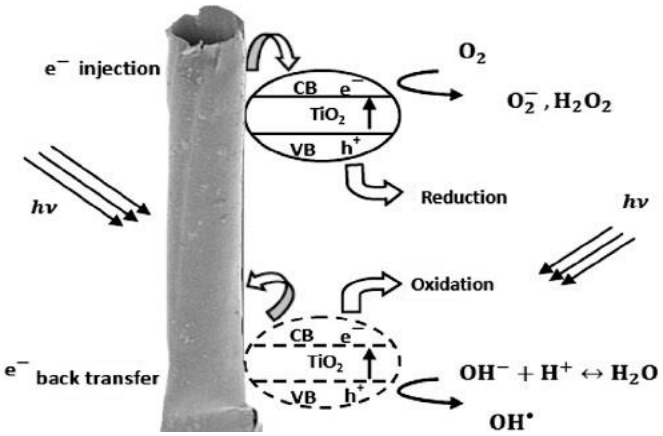

Fig. 5 Diagram of photocatalytic degradation of rhodamine B by activated carbon tube/TiO2 composite

Firstly, when the composite material is illuminated, electron-hole pairs are generated on the surface of TiO_2: $TiO_2 + hv \rightarrow e^- + h^+$;Subsequently, hydroxyl radicals are generated by the interaction between holes and water: $H_2O + h^+ \rightarrow \cdot OH + 2H^+$. Next, both hydroxyl radicals and holes can oxidize rhodamine B, and finally decompose into carbon dioxide and water: $\cdot OH$+ org(rhodamine B) $\rightarrow \cdots\cdots \rightarrow CO_2 + H_2O$; H^+ + org(Rhodamine B) $\rightarrow \cdots\cdots \rightarrow CO_2 + H_2O$

In this process, because the activated carbon tube can rapidly transfer electrons, its existence makes the adsorption of reactants and desorption of products proceed very fast, so the photocatalytic reaction rate is only determined by the surface reaction. The rate can be obtained from the following formula: $V = k\theta_b\theta_{OH}$ (1).In the equation, K is the surface reaction rate constant,θ_b is rhodamine B's coverage on the surface of TiO_2, and OH- is · OH coverage on the surface of TiO_2.In the system, $\theta_{OH\cdot}$ can be considered unchanged, the product adsorption is weak, so θ_b can be obtained by Langmuir formula, equation (1) can be changed to: $1/ = 1/kK_b \cdot 1/C_b \cdot 1/k$, where K_b is Rhodamine B adsorption equilibrium constant on the surface of TiO_2, C_b is the concentration of rhodamine B. The above equation is the Langmui Hinshelwood kinetic equation of the photocatalytic reaction, indicating that the relationship between $1/V$ and $1/C_b$ follows a straight line.

4. Conclusion

In this experiment, activated carbon tube /TiO_2 composite material was successfully prepared. The morphology and particle size of the powder products were controllable. The penetration of activated carbon tube not only increased the specific surface area of the material, but also played the role of electron transfer, further improving its photocatalytic performance. Calcination temperature is 580℃ C/ TiO_2 composite powder activated carbon tube, average particle size is small, the temperature for the preparation of TiO_2 did not happen by anatase rutile phase shift, and the simulation of pollutants of rhodamine B photocatalytic experiment, 140 minutes degradation rate can reach 100%, specifies that the preparation of the composite material has good photocatalytic performance.

References:

[1] P. Teszlak, M. Kocsis , A. Scarpellini ,et.al. Foliar exposure of grapevine to TiO_2 nanoparticles under field conditions: Photosynthetic response and flavonol profile. Photosynthetica, 2018, 56 (4): 1378-1386.

[2] B. J. Cong , J. Wang , J. Wang , et al. Cylindrical TiO_2 thin films prepared by sol-gel method and their photocatalytic properties . Journal of Vacuum Science and Technology , 2014,34 (09) : 938 - 942.

[3] R. J. Pan, Y. C. Wu. Deposition modification and physical properties of TiO_2 nanotube arrays. Hefei : Hefei University of Technology Press , 2012,2

[4] Y. Yuan, X. Qian, H. Han, et al. Synthesis of carbon modified TiO_2 photocatalysts with high photocatalytic activity by a facile calcinations assisted solvothermal method. J Mater Sci. 2017，28: 10028–10034.

[5] Chen Shunsheng , Cao Xin , Chen Chunhui , et al. Research progress of TiO_2 - based composite photocatalysts. Functional materials , 2018,49 (07) : 7039 -7049 + 7056

[6] K. Kun , Q. Z. Zhang . Nanometer titanium dioxide photocatalytic technology and air pollution control . China environmental science , 2018,38 (3) : 852 - 861

[7] J. Zhou, H. Wu, C. Y. Sun, et al. Ultrasmall C-TiO_{2-X} nanoparticle/g-C_3N_4 composite for CO_2 photoreduction with high efficiency and selectivity. J Mater Chem A. 2018, 43 (6):21596-21604.

[8] Z. Zhou , L. Li , S. L. Li. Preparation and photocatalytic properties of # titanium dioxide-carbon nanotube composites . Plastic additives , 2017 (03) : 27 - 31 .

[9] S. G .Du , J. Yan , M. Q. Wang, et al. Preparation of nano-TiO_2 / carbon nanotube composite particles and photocatalytic degradation of TNT wastewater . Energetic materials , 2014,22 (6) : 862 - 866.

[10] L. Y. Hu, Y. M. Zhang, S.M. Zhang, et al. A transparent TiO_2–C@TiO_2–graphene freestanding film with enhanced visible light photocatalysis. RSC Adv. 2016, 6, 43098.

[11] H. Lv, G. H. Zhang, C. P. Hao, et al. Activity of IrO_2 supported on tantalum-doped TiO_2 electrocatalyst for solid polymer electrolyte water electrolyzer. RSC Adv. 2017, 7, 40427-40436